Supporting Information

Ahmad et al. 10.1073/pnas.1111220108

SI Text

Protein Expression, Purification, and Activity Assay. ***Plasmid constructs.*** Plasmids pET-22b(+)-DnaJ and pET-22b(+)-DnaK containing ampicillin resistance gene were used in entire study. DnaJ 1–605, a DnaJ1–70 construct with His-tag on C terminus and required mutations were constructed with deletion, insertion, or point mutation techniques using the QuickChange mutagenesis kit from Qiagen. Briefly, primers were designed corresponding to the desired constructs followed by PCR amplifications using pfu-Ultra DNA polymerase (Qiagen). The product was digested using Dpn1 enzyme (Qiagen) to get rid of the parent plasmid. XL1-blue supercompetent cells (Qiagen) were transformed with the plasmid solutions obtained following manufacturer's protocol. Plasmid purification was carried out with the PureLink plasmid purification kit (Invitrogen). Purified plasmid was sequenced at University of Michigan DNA core facility.

Expression and purification. A fresh transformation of BL21 (DE3) singles competent cells (Novagen) with the desired plasmid was carried out each time a protein was expressed and purified. An LB, M9-N^{15}, M9-N^{15} C^{13}, or M9-N^{15} C^{13} D_2O 1 L media was inoculated with transformed cells and incubated at 37 °C. The media was induced after reaching an OD_{600} of 0.5 with 0.5 mM IPTG and was let grow overnight or 6 h at 37 or 30 °C according to standardized conditions for each construct/condition in our lab. Cells were harvested by centrifugation at 8,000 × *g* for 25 min. Harvested pellet was lysed with a French press. The lysed mixture was centrifuged at 30,966 × *g* for 30 min and the supernatant was loaded on a preequilibrated Ni-nitrilotriacetate (Invitrogen) column. The column was washed with at least two column volumes of Tris buffer A + NaCl-imidazole (Tris 25 mM, KCl 10 mM, PMSF 50 μM, NaCl 1 M, imidazole 10 mM, pH 7.4; $MgCl_2$ was not added in the case of DnaJ), followed by three column volumes of Tris buffer. The protein was eluted with 300 mM immidazole in the same buffer but at pH 8.0. The eluted protein was collected in tubes containing 5 mM EDTA (final conc.) to inhibit proteolysis by thermolysin. The purity of the protein was established by SDS-PAGE. Pure fractions were pooled, dialysed against pH 7.4 Tris buffer, and concentration determined. We used bicinchoninic acid for DnaK and Bradford's reagent for DnaJ.

Malachite green ATPase assay. Malachite green (0.0815% wt/vol): Polyvinyl alcohol (2.32% wt/vol): ammonium heptomolybdate tetrahydrate: ddH_2O were mixed in 2:1:1:2 ratio (vol/vol) and prepared fresh before every use. Ten microliters of DnaK (desired concentration) in Tris buffer A was placed in the wells of a 96-well plate (1). Similar or varying concentrations of DnaJ in a volume of 5 μL in Tris A buffer were added to each well followed by addition of 10 μL of 2.5 mM ATP in the same buffer. The plate was shaken in a plate shaker to ensure complete mixing and incubated for the desired time at 37 °C, after which 80 μL of Malachite green reagent was added to each well. The reaction was stopped at the desired time points by adding 10 μL sodium citrate (32% wt/vol) to each well. The wells were read after 15 min for absorbance at 620 nm on Spectramax5 Molecular Devices plate reader. Buffer replaced either of the components DnaK, DnaJ, or ATP in control experiments.

Kinetics of DnaJ–DnaK binding. The line broadening data in Fig. 3 in the text were used to estimate the kinetics of the DnaJ–DnaK binding. A reasonable fit to the data was obtained when using the equation for intermediate/fast exchange line broadening,

$$R_2 = f_{\text{free}} R_2^{\text{free}} + f_{\text{bound}} R_2^{\text{bound}} + \frac{f_{\text{free}} f_{\text{bound}} \Delta\omega^2}{k_{\text{ex}}},$$

where a K_D of 16 μM obtained from the chemical shift changes (Fig. S1) was used to calculate f_{free} and f_{bound}, while fitting on $\frac{\Delta\omega^2}{k_{\text{ex}}}$ and R_2^{bound}.

The average squared ^{1}HN chemical shift change $\Delta\omega^2$ for the titration is found to be 350 $\text{rad}^2\,\text{s}^{-2}$, leading to $k_{\text{off}} = 14\ \text{s}^{-1}$ from the fit.

NMR relaxation. Standard ^{15}N R_1 and R_2 experiments were recorded using the 800-MHz spectrometer, using a 300-μM sample of DnaJ(1–70) in the absence or presence of 300 μM DnaK. The average relaxation rates are listed in Table S1. At the mixed conditions, DnaJ(1–70) is bound for 73% of the time to DnaK (using a K_D of 16 μM). Because the binding process is in fast exchange with only very small exchange broadening, we may extrapolate the obtained ^{15}N relaxation rates to the 100% bound case as shown in Table 1.

We fitted the relaxation data of bound DnaJ using the Model-free paradigm. The use of this approach is justified as follows. From the NMR titration, we obtain a k_{off} of 14 s^{-1}. The k_{off} is much slower than the rotational correlation time; therefore, DnaJ, when fully bound to DnaK, has NMR relaxation properties that are dominated by the rotational correlation times and not kinetics. For NMR relaxation, this system does not behave differently from, e.g., a floppy C-terminal tail of a protein. The Model-free parametrization is valid for a relaxation vector that moves independently, but restricted, from a (not necessarily larger) body. The raw ^{15}N relaxation data of DnaJ(1–70) bound to DnaK (1–605) shows that each DnaJ(1–70) NH (amide proton) relaxation vector reorients approximately 5 times faster than the DnaK molecule itself. The difference in correlation times also follows from the calculations below. With that difference in timescale and in size of the molecules, the assumption of independent motion is reasonable.

Because the J domain happens to be an α-helical bundle, most NH vectors in DnaJ(1–70) point in the same direction (parallel to the helical axes). Hence the average order parameters of these vectors describe the average order parameter of the DnaJ domain itself, and Model-free can be used to describe the motion of DnaJ(1–70) with respect to DnaK.

Our data show that the presence of DnaJ(1–70) does not affect the intensities of the resonances of DnaK nucleotide-binding domain (NBD), substrate-binding domain (SBD), or linker. Therefore, DnaK's NBD and SBD move independently in the complex, just as in the free molecule (2). Because DnaJ (1–70) is predominantly tethered to the NBD, the overall correlation time as experienced by J70 is dominated by the rotational correlation time of the NBD in the context of the full complex. This correlation time was determined in previous work (2) and is 28 ns. We may assume close to isotropic overall motion of the NBD-J70. In this limit, Model-free is completely valid.

The data were first fitted using the density function (3)

$$J(\omega) = \frac{S^2 \tau_C}{1 + (\omega\tau_C)^2} \qquad \textbf{[S1]}$$

for both R_1 and R_2, together with an R_{ex} exchange term for R_2. We used an in-house written grid-search program. A fit to the

extrapolated data yielded $\tau_c = 8.0$ ns for DnaJ(1–70) 100% bound to the 70 kDa DnaK (see Table S1). This result shows that J70 moves around quite freely while it is stoichiometrically and saturably bound to DnaK, given that the rotational correlation time for DnaK by itself is 28 ns (3). We call this phenomenon "tethered binding."

We imposed an overall correlation time of 28 ns (see above) and fitted the data with the density function (3)

$$J(\omega) = \frac{S^2\tau_C}{1+(\omega\tau_C)^2} + \frac{(1-S^2)\tau}{1+(\omega\tau)^2}, \qquad \textbf{[S2]}$$

where

$$\frac{1}{\tau} = \frac{1}{\tau_C} + \frac{1}{\tau_e},$$

and where τ_e is the correlation time of DnaJ(1–70) in the complex.

As Table 1 shows, this fit returns $S^2 = 0.37$ and a value of 3.8 ns for τ_e, which is close to the value of τ_c for free DnaJ(1–70).

We note that the estimation of $S^2 = 0.37$ should be viewed as an upper limit: If the assumption that NBD and SBD remain as freely tethered as in DnaK by itself is not valid, the overall correlation time would become larger. Also, the motion would become anisotropic, which leads to a further increase of correlation time (rigorously true for all directions in an ellipsoid). Due to both effects, the order parameter needed to fit the relaxation data of DnaJ in the complex would become lower.

We calculated the order parameter for a variety of overall correlation times, as shown in Table S1. The table shows that a fit with the lowest value for R_{ex} and a physically reasonable value for τ_e is indeed obtained around $\tau_c = 28$ ns, lending much credence to the validity of our assumptions.

If the motion of DnaJ(1–70) with respect to DnaK can be described as tethered to one point and moving around in a cone with respect to that point, one obtains from ref. 3 for $S^2 = 0.37$

$$S^2 = \left\{\frac{\cos\theta(1+\cos\theta)}{2}\right\}^2$$

an angle of 45° for θ, the half-opening angle.

1. Chang L, et al. (2008) High-throughput screen for small molecules that modulate the ATPase activity of the molecular chaperone DnaK. *Anal Biochem* 372:167–176.
2. Bertelsen EB, Chang L, Gestwicki JE, Zuiderweg ERP (2009) Solution conformation of wild-type E. coli Hsp70 (DnaK) chaperone complexed with ADP and substrate. *Proc Natl Acad Sci USA* 106:8471–8476.
3. Lipari G, Szabo A (1982) Model-free approach to the interpretation of nuclear magnetic-resonance relaxation in macromolecules. 2. Analysis of experimental results. *J Am Chem Soc* 104:4559–4570.

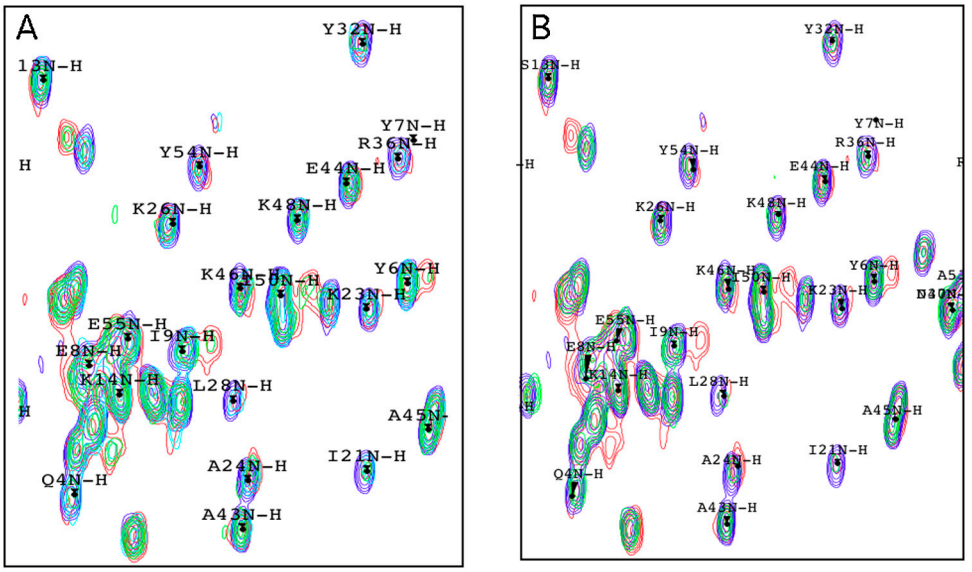

Fig. S1. (*A*) ^{15}N-^{1}H transverse relaxation-optimized spectroscopy of DnaJ(1–108) upon addition of DnaK(1–605) in the absence of NRLLLTG (J:K) ratio: (1:0) blue, (1:0.5) cyan, (1:1) green, (1:2) red. (*B*) The effect of adding NRLLLTG to the sample of the J:K complex. (J:K) ratio (1:0) blue, (1:2 no NRLLLTG) red, (1:2 + NRLLLLTG) green.

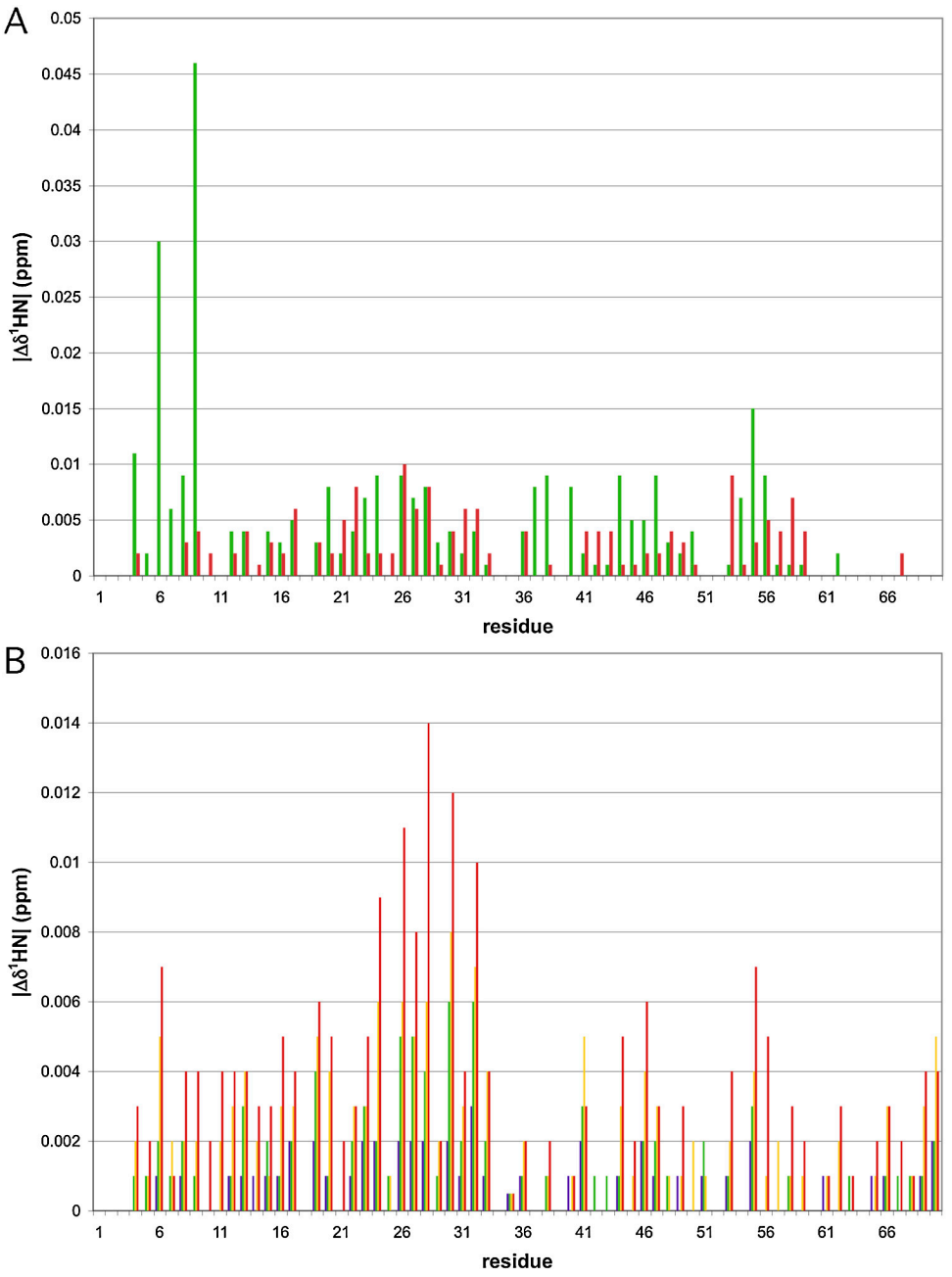

Fig. S2. (*A*) Histogram of chemical shifts in DnaJ(1–108) upon addition of DnaK(1–605) (green). In red, the remaining shifts after addition of NRLLLTG to that sample. (*B*) Stepwise titration of DnaJ(1–70) with DnaK(1–605) in the presence of NRLLLTG (DnaJ:DnaK ratios 1 : 0.25, 1 : 0.50, 1 : 1, 1 : 2 following rainbow colors from blue to red).

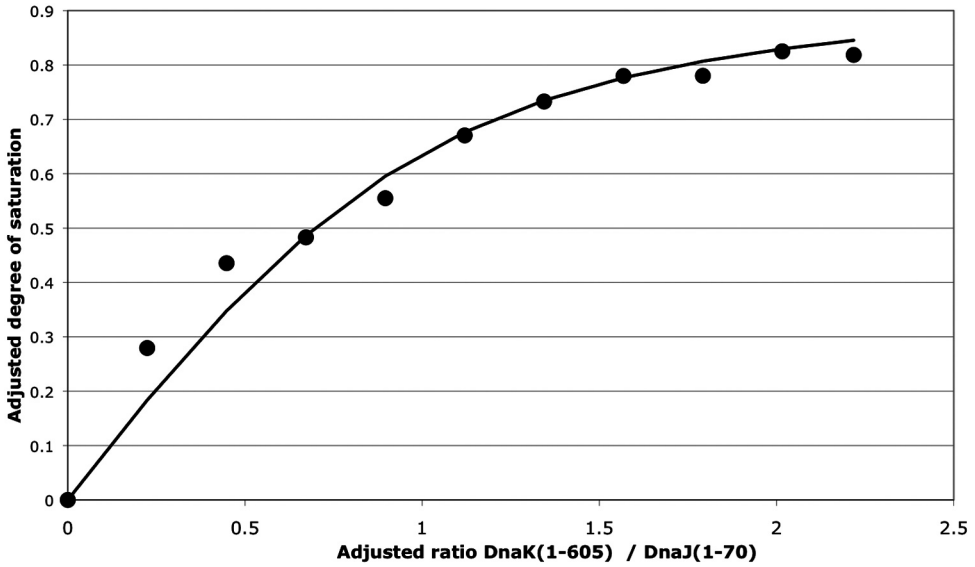

Fig. S3. Isotherm for the binding of DnaK(1–605) to DnaJ(1–70) as monitored with a $^{1}H^{15}N$ transverse relaxation-optimized spectroscopy spectrum of DnaJ. The data points are averages of the chemical shift changes for all residues. The result is $K_D = 16$ μM.

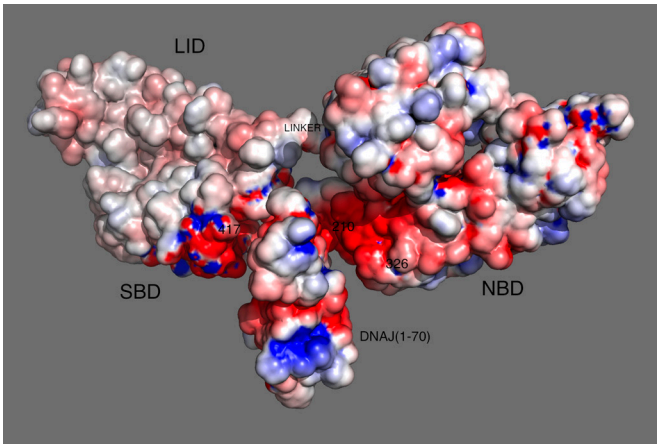

Fig. S4. Poisson–Boltzmann electrostatic surface charges in the complex of DnaK(1–605) and DnaJ(1–70). The surface charges are contoured between −8 kT (red) and +8 kT blue). The figure was prepared in Pymol, using the plug-in written by Carlson and Delano. The location of the spin labels V210C-MTSL [S-(2,2,5,5-tetramethyl-2,5-dihydro-1H-pyrrol-3-yl)methyl methanesulfonothioate], D326C-MTSL, and T417C-MTSL are indicated. Residues representing domains of DnaK: NBD 1–383; Linker 384–396; SBD 397–507; LID 508–602.

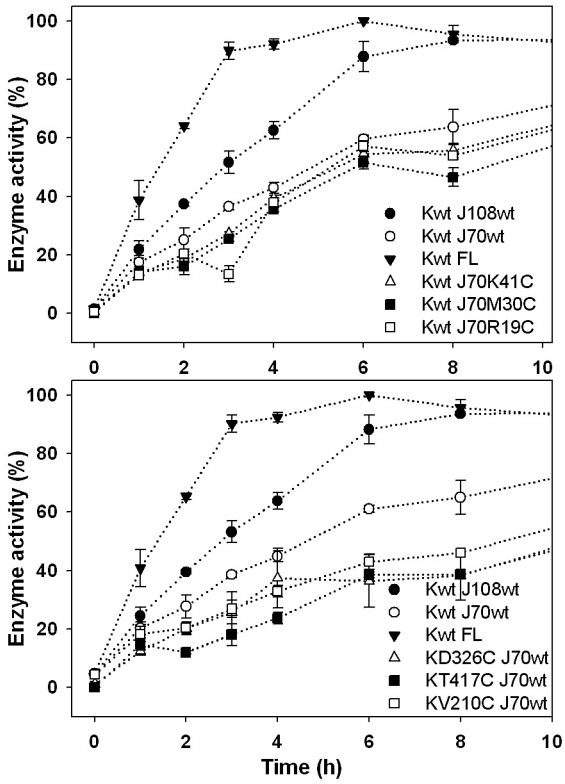

Fig. S5. Stimulation of the ATP hydrolysis of different mutants of DnaK in the presence of various amounts of DnaJ(1–108) and DnaJ(1–70) and NRLLLTG. The assay quantitates the formation of inorganic phosphate, detected by change in absorbance of malachite green. FL, full-length DnaJ wild type.

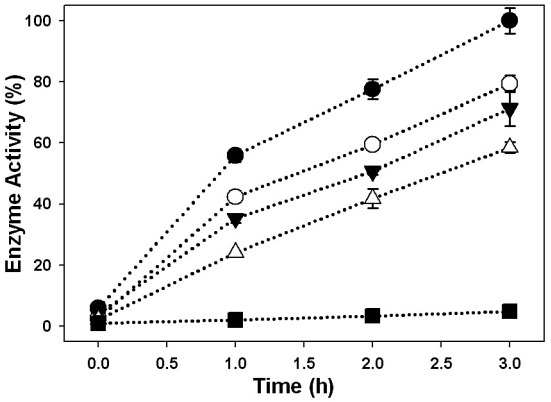

Fig. S6. Malachite green assay on Mutants Enzyme activity monitored by the release of phosphate in ATP hydrolysis by DnaK as a function of time. (●) DnaK1–605 WT + DnaJ1–70 WT; (○) DnaK1–605_D208A/E209A + DnaJ1–70 WT; (▲) DnaK1–605_D208A/E209A; (△) DnaK1–605 wt; (■) DnaJ1–70 WT. All samples contained 50 μM peptide, 500 μM ATP, 2 μM DnaK, and 10 μM DnaJs.

Table S1. Model-free fitting data for the ^{15}N relaxation of DnaJ(1–70) free and bound to DnaK

	τ_c, ns	$J(\omega)$	$\langle R_1\rangle_{exp}$, s^{-1}	$\langle R_1\rangle_{fit}$, s^{-1}	$\langle R_2\rangle_{exp}$, s^{-1}	$\langle R_2\rangle_{fit}$, s^{-1}	$\langle R_{ex}\rangle_{fit}$, s^{-1}	$\langle S^2\rangle_{fit}$	$\langle \tau_e\rangle_{fit}$, ns
J-70 free	5.2*	Eq. **S1**	1.39	1.39	10.68	10.68	2.7	0.80	—
J-70 73 % bound	7.0*	Eq. **S1**	1.123	1.123	24.06	24.06	13.3	0.82	—
J-70 100% bound	8.0*	Eq. **S1**	1.02	1.02	28.98	28.98	16	0.85	—
J-70 100% bound	12.0†	Eq. **S2**	1.02	1.02	28.98	28.98	7.22	1.00	0.89
J-70 100% bound	16.0†	Eq. **S2**	1.02	1.02	28.98	28.99	7.44	0.71	2.86
J-70 100% bound	20.0†	Eq. **S2**	1.02	1.02	28.98	29.01	8.88	0.51	3.00
J-70 100% bound	24.0†	Eq. **S2**	1.02	1.02	28.98	28.98	7.08	0.45	3.53
J-70 100% bound	**28.0**†	Eq. **S2**	**1.02**	**1.02**	**28.98**	**28.98**	**6.86**	**0.37**	**3.83**
J-70 100% bound	32.0†	Eq. **S2**	1.02	1.02	28.98	28.98	5.66	0.28	6.68
J-70 100% bound	36.0†	Eq. **S2**	1.02	1.02	28.98	29.04	7.26	0.17	9.01
J-70 100% bound	40.0†	Eq. **S2**	1.02	1.01	28.98	29.05	9.08	0.12	8.68
J-70 100% bound	44.0†	Eq. **S2**	1.02	1.00	28.98	28.92	15.34	0.14	1.46
J-70 100% bound	50.0†	Eq. **S2**	1.02	1.02	28.98	28.92	13.26	0.16	0.75

*S^2 and τ_c determined by the fit to Eq. **S1**.
†S^2 and τ_e determined by the fit to Eq. **S2**, τ_c imposed.

Table S2. Sequence alignment for the DnaJ–DnaK contact region of DnaK *Escherichia coli* with the seven major human heat shock proteins 70 kDa (HSPA)

		204	205	206	207	208	209		210	211	212	213	214	215	216	217	218	219	220	221	222	223
DnaK	DnaK *E. coli*	I	I	E	I	D	E	—	V	D	G	E	K	T	F	E	V	L	A	T	N	G
HSPA1A	Hsp70 1A/1B	I	L	T	I	D	D	G	I	—	—	—	—	—	F	E	V	K	A	T	A	G
HSPA1L	Hsp70 1-like	I	L	T	I	D	D	G	I	—	—	—	—	—	F	E	V	K	A	T	A	G
HSPA2	Hsp70 2	I	L	T	I	E	D	G	I	—	—	—	—	—	F	E	V	K	S	T	A	G
HSPA5	Bip	L	L	T	I	D	N	G	V	—	—	—	—	—	F	E	V	V	A	T	N	G
HSPA6	Hsp70 6	V	L	S	I	D	A	G	V	—	—	—	—	—	F	E	V	K	A	T	A	G
HSPA8	Hsc70	I	L	T	I	E	D	G	I	—	—	—	—	—	F	E	V	K	S	T	A	G
HSPA9	mt-Hsp70	I	L	E	I	Q	K	G	V	—	—	—	—	—	F	E	V	K	S	T	N	G
		209	210	211	212	213	214	215	216						217	218	219	220	221	222	223	224

E. coli count is at the top; human HSPA8 count at the bottom. Shaded areas indicate beta strands.

Table S3. Paramagnetic relaxation enhancement constraints used in the molecular dynamics calculation

Constraint	Range, Å
Val210 CG1 → DnaJ(10–12,17–25,33–36,49–58)HN	15–20
Val210 CG1 → DnaJ(26–31)HN	5–15
Val210 CG1 → DnaJ(others)HN	20–200
Asp326 CG → DnaJ(26–31)HN	15–20
Asp326 CG → DnaJ(others)HN	20–200
Thr417 OG1 → DnaJ(26–31)HN	15–20
Thr417 OG1 → DnaJ(others)HN	20–200
Asp148 OG1 → DnaJ(all)HN	20–200
Lys166 CD → DnaJ(all)HN	20–200
Lys421 CD → DnaJ(all)HN	20–200
Lys421 CD → DnaJ(all)HN	20–200
DnaJ Met30 CE → DnaK(211)HN	5–10
DnaJ Met30 CE → DnaK(206–210,212–221)HN	5–15
DnaJ Met30 CE → DnaK(others)HN	20–200
DnaJ Arg19 CD → DnaK(all)HN	20–200
DnaJ Lys41 CD → DnaK(all)HN	20–200